Available online at www.sciencedirect.com

ScienceDirect

Procedia CIRP 104 (2021) 1412–1417

www.elsevier.com/locate/procedia

54th CIRP Conference on Manufacturing Systems

Study of the influence of the hardening rule on a multi-step global manufacturing process modeling.

Diego Britez [a]*, Sana Werda [a], Raynald Laheurte [a], Philippe Darnis [a] and Olivier Cahuc [a]

[a] *Université de Bordeaux, CNRS, ENSAM, I2M Bordeaux, 351 cours de la Libération, Talence, France*

* Corresponding author. Tel.: +33-7-68 87 34 41. *E-mail address:* diego-luis.britez-gonzalez@u-bordeaux.fr

Abstract

Energy consumption during manufacturing is a key element for the environmental impact assessment in modern industry. In order to optimize and avoid undesirable residual deformations in the final product in an overall manufacturing process, it is necessary to correctly identify the variables that describe the state of the matter. This will allow to recreate the interaction existing between the individual process in the global chain. Numerical simulations results of a chain of combined solicitations, using different hardening rules for the same material, show the importance of this choice when the simulation of successive processes is foreseen.

Keywords: process chain simulation; anisotropic evolution; strain hardening, multi-step multiaxilal loading.

1. Introduction

Over of the last decades the computational capacity has evolved in a considerable way, the advances of numerical simulation models of manufacturing processes have accompanied this progress and evolved at the same time. Optimizations based on real time machinery and product flow big data acquisition are is the main characteristic in the fourth industrial revolution era [1,2].

Numerical simulations help to reduce the number of experimental tests and to optimize independent and the global manufacturing chain process. They are also a tool to study the nature of the phenomena and changes that occur during plastic deformation and manufacturing processes.

This work focus on the problem of the processes interaction from a physical point of view, in order to follow the material. When a different hardening rule is used, other state variables are required, which indeed will have a major influence for a multiple operations global process simulation.

In order to optimize a global manufacturing process it is necessary identify the variables that characterize the state of each point of the material. This action will allow assuring the traceability of the process.

The present work proposes the study of the influence of the hardening rule adopted in the formulation of the behavior law to evaluate its influence on the global manufacturing production.

The main long-term goal of this work is to model the behavior of the work piece all along the manufacturing process. Taking into account that the actual strategy to control processes interaction is to eliminate undesirable internal stresses by annealing, gaining a prediction capacity would allow not only to control the processes parameters avoiding highly energetic operations but also a new tool to re design the overall manufacturing process.

The bibliographic background of this work is divided in three sections: the state of the art, the theoretical framework and the classification of the phenomenological hardening rules applied to the formulation of the behavior laws. Then a simple benchmark example is applied by using two different hardening rules. The benchmark example is followed by an analysis of the results exposing the principal limitation of the isotropic hardening rule when multi-step loading is carried on. Finally, the outlook and perspectives of the work are presented.

2. State of the art

The beginning of the study of the overall manufacturing process, its simulation as well the industrial design and optimization is dated in the year 1777 with the Monte Carlo

10.1016/j.procir.2021.11.238

simulation methodology. From this moment different industrial eras has been passed to the actuality that can be considered as the fourth industrial revolution or the digitalized era. A complete bibliographical review of the manufacturing evolution design optimization are found in [3,4].

Nevertheless, industrial optimization topics are based on virtual factory simulation, planning and verification, manufacturing systems and networks planning and control, material and information flow design, factory layout design [3]. The material properties control has always been seen as a quality parameter but rarely taken into account as an overall manufacturing optimization parameter.

The first fundamental research looking to predict the behavior of a sheet rolled metallic plate was carried out by [5], this proposed behavior law is variation of the Von Mises yield limit where the yield properties are affected by the lamination direction. This law does not explain the anisotropic evolution of the material properties from the annealed state.

The first experimental studies studying the anisotropic evolution of the yield surface from its annealed state where carried by [6, 7] showing similar results.

The most important phenomenological characteristic for a limited number of loading steps (< 10) at low temperature is the Bauschinger effect that can be characterized by a kinematic hardening rule[8], in these cases ratcheting and dynamic recovery effects may be neglected.

Despite these important conclusions most of the works considering a multiple process chain simulation are isotropic hardening law based [9–12].

Recently [13] demonstrated the influence of the hardening rule on final plastic strains after a multistep loading process. This work analyses the energetic differences in the predicted results as well.

3. The continuum mechanics and thermodynamic coupled frame

Considering a transformation of the state of the material as a change on the thermodynamic state has a considerable advantage. The thermodynamic state is a defined condition that is fully identified by a set of parameters known as the thermodynamic state variables. With the knowledge of these variables the trace of the evolution of the metal state all along the transformation history is possible.

By coupling continuum mechanics framework and thermodynamics laws it is possible to derive to constitutive behavior laws[14]. This point of view of the problem was proposed by Germain[15] and later applied on many formulations i.e. [16–18].

The elements that compose this framework are:

- **The Helmholtz free energy** ψ: is the energy associated to the thermodynamic variables(α_i) that describe the hardening phenomena. A variation of the free energy is given by [17–19]:

$$d\psi = \frac{\partial \psi}{\partial T} dT + \frac{\partial \psi}{\partial \alpha_i} d\alpha_i \qquad (1)$$

where α_i represent the i_{th} thermodynamic variable used in the model and is linked to its corresponding strain hardening variable A_i by:

$$A_i = \frac{\partial \psi}{\partial \alpha_i} \qquad (2)$$

- **The load function** $f(\sigma, A_i)$: is the function that delimits the elastic frontier. When the set of hardening variables verify the condition:

$$f = 0, \qquad (3)$$

the load is found on edge of the elastic limit, the hypersurface that verifies this condition is known as the elastic threshold. The load function cannot take values greater than 0, so when an external solicitation is found outside of the elastic domain will force a change of the hyper-geometry of the elastic threshold, it may vary the position, the size, or the shape of it. This evolution is controlled by the **consistency condition** given by:

$$df = 0, \qquad (4)$$

- **The flow potential** $F(\sigma, A_i)$: it is also a function of the stress field and the hardening variables. It defines the intensity of the strain hardening and the thermodynamic variables rate through the application of the **hardening rule** given by:

$$\begin{aligned} d\tilde{\varepsilon}^p &= \frac{\partial F}{\partial \tilde{\sigma}} d\lambda, \\ d\alpha_i &= \frac{\partial F}{\partial A_i} d\lambda, \end{aligned} \qquad (5)$$

where λ is a scalar known as the plastic multiplier.

The set of equations 1-5 are capable to fully characterize and define a specific state of the matter during plasticity.

For elastic transitions, the Hooke's law can be applied to complete the given set.

4. Behavior laws classification

Behavior laws may be classified by the adopted hardening rule, isotropic, kinematic, combined, and anisotropic. Each family is characterized with a specific hardening variable or set of variables (with the exception of the anisotropic family that may include non-conventional hardening variables).

Isotropic hardening laws are characterized by a scalar hardening variable (usually represented by R). In this particular family, hardening evolves evenly in all directions when the initial elastic threshold is exceeded, so it may be interpreted as an expansion of the elastic domain [20, 21]. Therefore, it is not possible to model some phenomena that could have a relevant importance in the simulation of the manufacturing process chain interaction, such as the generalized Bauschinger effect.

The kinematic hardening rules model the strain hardening phenomena as a translation of the elastic threshold instead of an expansion. The coordinates of the center of the elastic domain represents the hardening variable (a tensor usually represented by $\tilde{X}$)[17, 20–23]. This kind of modelling allows reproducing the Bauschinger effect and ratcheting effect on cyclic loads. A review and evaluation of different kinematic hardening rules are given on [22, 24]. The translation of the elastic threshold induces an anisotropy on the state of the material.

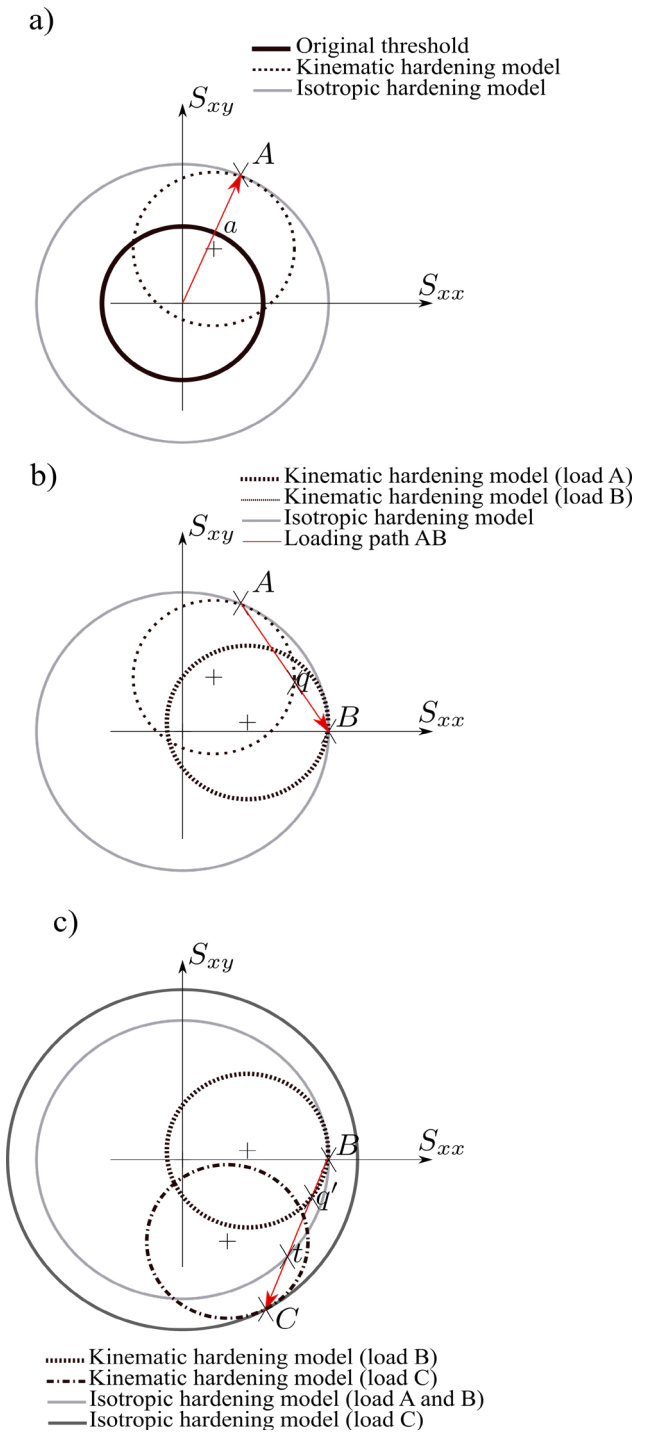

Fig. 1. Load sequence scheme in the isotropic and kinematic hardening model on deviatoric coordinates. 1a) Load A. 1b) Load B. 1c) Load C

The combined hardening rule refers to the use of kinematic and isotropic hardening variables. The use of both variables allows to reproduce cyclic hardening and softening which is not possible by using only one hardening rule [20–22].

Experimental studies show that a more complex hardening rule is needed to accurate reproduce the strain hardening effects such as cyclic hardening and softening, ratcheting effect, etc. [20–22, 25, 26] .

The more realistic model, an anisotropic deformation of the elastic threshold is found during a plastic deformation. The loading direction plays a major role in the adopted shape. Only a few number of these models i.e. [18,26] included the presented thermodynamic framework in the formulation. Further studies are needed in order to evaluate if their application show relevant differences in relation to kinematic or combined models predictions.

5. A benchmark problem

5.1 Problem statement

In order to show the influence of the hardening rule on the results obtained after a chain of multiple loading steps, the parameters of an isotropic and a kinematic laws presented on table 1 are considered, where $\tilde{S}$ is the stress field represented in the deviatoric space:

$$\tilde{S} = \tilde{\sigma} - \frac{tr(\tilde{\sigma})}{3}\tilde{I}, \qquad (6)$$

where elastic strains are calculated using the Hooke's law with an elasticity modulus of $E = 200\ (GPa)$ and Poisson coefficient equal to $\nu = 0.3$.

Table 1. Behaviour constitutive equations. Extracted from [21]

Isotropic model	
Strain decomposition	$\tilde{\varepsilon} = \tilde{\varepsilon}^e + \tilde{\varepsilon}^p$
Load function	$f(\tilde{\sigma}, R) = J_2(\tilde{S}) - \tilde{\sigma}_0 - R \ with\ \ J_2(\tilde{S}) = \sqrt{\frac{3}{2}\tilde{S}:\tilde{S}}$
Flow potential	$F(\tilde{\sigma}, R) = J_2(\tilde{S}) - \sigma_0 - R - \frac{R^2}{2Q}$
Free energy	$\psi = \frac{1}{2}bQr^2$
Model Parameters	$Q = 150\ (MPa); b = 50; \sigma_0 = 100\ (MPa)$
Kinematic Model	
Strain decomposition	$\tilde{\varepsilon} = \tilde{\varepsilon}^e + \tilde{\varepsilon}^p$
Load function	$f(\tilde{\sigma}, \tilde{X}) = J_2(\tilde{S} - \tilde{X}) - \sigma_0$ $with\ J_2 = \sqrt{\frac{3}{2}(\tilde{S} - \tilde{X}):(\tilde{S} - \tilde{X})}$
Flow potential	$F(\tilde{\sigma}, \tilde{X}) = J_2(\tilde{S} - \tilde{X}) - \sigma_0 + \frac{\gamma}{2C}J_2^2\ (\tilde{X})$ $with\ \ J_2(\tilde{X}) = \sqrt{\frac{3}{2}\tilde{X}:\tilde{X}}$
Free energy	$\psi = \frac{1}{3}C\,\tilde{\alpha}:\tilde{\alpha}$
Model Parameters	$C = 7500\ (MPa); \gamma = 50; \sigma_0 = 100\ (MPa)$

A particle is submitted to three different consecutive loadings steps, no load release is made between each load. The loading history is summarized on table 2:

Table 2. Loading steps description (Units given in MPa)

	σ_{xx}	τ_{xy}	σ_{eq}
Step A	75	75	150
Step B	150	0	150
Step C	80	-80	160

where, σ_{eq} refers to the Von Mises equivalent stress.

5.2 Domain of validity

The domain of validity is limited by the hypotheses taken in adopted behavior and the test conditions. For the particular case of the problem developed in this work the following considerations are taken into account [21]:

1. Constant temperature.
2. Damage absence.
3. Absence of viscous term (time independent solution).

5.3 Results and analyses

Table 3 presents the total strains obtained after each loading step, while on table 4 the plastic strains as well cumulated plastic strain (p_{cum}), calculated with both considered behavior rules.

During the step A no difference is noted on the response stress vs. strain, however the modelling on strain hardening brings an important consequence for later stages.

Figure 1a) helps the comprehension through a schema. Both models predict yielding at the same moment when the load reaches the elastic threshold at point *a*. The final solution (strains, energy and cumulated free energy) is similar in this case only because yielding occurs at same moment and at the same point.

The last case is going to be true only for an annealed state, free of hardening effects. The residual properties of the metal affect the subsequent loads.

The load B has the same equivalent stress value of load A (*150 MPa*), consequently there is no yielding when isotropic model is used. This is clearly reflected on plastic strain values at the end of step B, where there is no change compared from those obtained on step A. On the other hand kinematic model yields when the loading reaches the elastic threshold at the point q on figure 1b).

Table 3. Total strains evolution along a multistep loading process modelled with an isotropic and kinematic hardening rule.

	Model	ε_{xx}	ε_{xy}
Step A	Isotropic	4.32E-03	6.43E-03
	Kinematic	4.32E-03	6.43E-03
Step B	Isotropic	4.75E-03	6.44E-03
	Kinematic	9.87E-03	5.36E-03
Step B	Isotropic	5.53E-03	4.22E-03
	Kinematic	1.44E-02	-3.28E-03

On step C (represented schematically in figure 1c) the load path BC intercepts to the kinematic threshold model on q' and the isotropic on t. Again, a longer portion of the load is on plasticity for the kinematic model compared to the isotropic. As one of the consequences, the final strain on the kinematic model exceeds the isotropic on 162% on the principal direction and they differ on the sign of the shearing direction.

Table 4. Plastic strains and cumulated strains evolution along a multistep loading process modeled with an isotropic and kinematic hardening rule.

	Model	ε_{xx}^{p}	ε_{xy}^{p}	p_{cum}
Step A	Isotropic	4.06E-03	6.08E-03	8.11E-03
	Kinematic	4.07E-03	6.12E-03	8.11E-03
Step B	Isotropic	4.06E-03	6.20E-03	8.20E-03
	Kinematic	9.37E-03	5.36E-03	1.35E-02
Step C	Isotropic	5.24E-03	4.54E-03	1.02E-02
	Kinematic	1.40E-02	-3.15E-03	2.46E-02

The predicted plastic energy developed during strain hardening also shows an important discrepancy between the two models as shown in table 5. The specific plastic energy developed during strain hardening is calculated by:

$$de_{plast} = \tilde{\sigma} : d\tilde{\varepsilon}^{p}, \qquad (7)$$

The kinematic hardening model predicts after the three loading steps a total specific energy of $3.22\ (Mpa.mm/mm)$ while the isotropic model only predicts $1.43\ (Mpa.mm/mm)$. Again, the difference between predictions is over 100%.

The dissipated energy is the difference between specific plastic energy developed during strain hardening and the free energy ψ[21], used to change the internal structure of the metal.

The identical results obtained during the first loading step (strains, plastic strains, specific energy and free energy consumption) in both models, helps to understand why so accurate predictions are made by using isotropic models on a single process simulation [27–30].

Table 5. Specific energy developed

	Model	$\tilde{\sigma} : \tilde{\varepsilon}^{p}$ $MPa.\frac{mm}{mm}$	$\Delta\psi$ $MPa.\frac{mm}{mm}$
Step A	Isotropic	1.03	0.17
	Kinematic	1.03	0.17
Step B	Isotropic	0	0
	Kinematic	0.72	0.08
Step C	Isotropic	0.34	0.073
	Kinematic	1.47	-0.09

The free energy ψ depends only on the thermodynamic variables, so it is independent of the load path. On the other hand, the dissipated energy ϕ, that is the thermic energy exchanged with the environment is defined as[21]:

$$d\phi = d\tilde{\sigma} : d\tilde{\varepsilon} - \rho d\psi, \qquad (8)$$

in this case, there is a dependency on the loading path as it is a function of the values obtained on each differential increment during plasticity.

The free energy is a storage mechanism within the metallic crystalline system [21]. From another point of view, the free energy emerges as result of applying the thermodynamic frame to a specific phenomenological model.

During the load A, the results of the variation of free energy in both models are identical (as well the developed strains), therefore the dissipated energy ϕ are also the same.

As the kinematic model is not represented by a scalar potential, the differences are going appear when the load direction and the normal of the elastic surface are no longer coincident (typical case of a no proportional load).

The kinematic model allows a reversibility of the thermodynamic state. This implies a release of the energy stored within the crystalline network. This phenomenon is reflected in negative values of the variation of the accumulated free energy during the process C.

Isotropic model is not capable to reproduce the generalized Bauschinger effect, so is expected its incapability to reproduce properly a chain of consecutive loadings. This also may be explained by the fact that isotropic model are based on monotonic tests, following a single direction load.

Furthermore, if the loading history forces the return to the elastic domain (typical during unloading), to be reloaded with a different direction, predictions lose any similarity.

Results show strain hardening and thermodynamic variables have a major importance on describing the state of the material.

Furthermore, manufacturing processes involving non-proportional loads will show similar limitations when using an isotropic model.

The kinematic model used in this work corresponds to the Amstrong and Frederick model[17]. According to *Portier et al*[24] it over estimates the Bauschinger effect. Further studies should be carried out to compare results obtained with different kinematic, combined, and anisotropic models. The residual stress field found on a work piece may be compared to the results of simulations performed with the different hardening rules as a methodology to evaluate the accuracy of each model.

6. Discution and outlook

The obtained results evidence two main points:

- The obtained results by using an isotropic or kinematic hardening rule (plastic strain, internal free energy and dissipated energy) are only going to be coincident when the loading path does not cross the elastic thresold once plasticty has been reached.
- If a loading cross the elastic threshold once plasticity has reached, the Basuchinger effect will cause difference in predictions. In the particular case of the numerical example developed in the previous section, differences are higher than 100% after three solicitations.

The results are obtained in similar conditions than [8], for a low number steps (<10), where experimental results show a good correlation with kinematic model of Chaboche. Based on this result it is possible to infer that the kinematic model show better results.

Future experimental works should be carried out in order to validate this hypothesis. Furthermore the influence of new parameters should be included such temperature and viscous terms.

The present work is useful in order to identify the influence of the hardening rule during a multi-step loading in a simple case (single element analysis) and how the loading history affects the final strain and energy.

The same methodology should be applied in order to simulate real operations manufacturing chain. It can be noticed that different operations may require different meshing requirements. In this case the hardening variables characterizing the state of the material (at the integration points) should be exported (i.e. interpolated or extrapolated) to the new interpolation points.

Previous work, where numerical simulations trace the state of the material from an initial annealed state through different operations, based on real operations, use an isotropic hardening rule in the behavior law formulation [9–12].

7. Conclusion

In spite of the industrial manufacturing optimization has been studied from the beginning of the first industrial revolution, the optimization of the overall process based on the control of the material properties was little studied.

The present study, together with those found in the references [8, 13] offer some key points to be taken into account when an overall simulation process is performed. Accurate models will allow generating precise results that can feed optimization algorithms.

An important difference in the predicted dissipated energy, free energy and the developed plastic strains when comparing isotropic and kinematic rule-based behavior laws during a multiple loading process were found.

In order to look for a methodology capable to ensure a traceability of the state of the matter along the entire manufacturing process, the evaluation of a hardening rule presented on thermodynamic framework is revised. The use of a behavior law in the thermodynamic frame allows establishing the relation between its thermodynamic state with its hardening state, assuring the unicity of the solution. So a defined state may be characterized by the stress, strains, and the hardening variables.

Isotropic behavior laws are obtained through monotonic tests with annealed test tubes; they are accurate defining the stress/strain evolution along one single loading path. The generalized Bauschinger effect cannot be reproduced with this family of hardening rule, conducing to thermodynamic state is not accurately defined. This situation leads to erroneous results when subsequent charges cross the elastic threshold (re-entering into elastic domain) on a multiple step loading, which represent the most general case on a multi-step manufacturing process.

The practical example developed in this work offers an idea about how different results can be when using different hardening rules.

In general, isotropic models will underestimate plastic strain hardening and dissipated energy on a multiple loading and non-proportional loading case.

Free energy and dissipation emerge as a consequence of using the thermodynamic framework. The heat production during a multiple load process can be measured and be taken in advantage to develop more accurate phenomenological models in the future.

Results must be compared with other hardening rules (kinematic, combined, and anisotropic) in order to evaluate the accuracy vs. cost of computation.

The present study does not take into account viscous, temperature and damage effects; further studies should be carried out to include these effects on the model, and the identification of the state variables to add in order to create more accurate phenomenological behavior laws.

References

[1] Mourtzis D, Vlachou E, Milas N. Industrial big data as a result of IoT adoption in manufacturing. *Procedia cirp* 2016; 55: 290–295.

[2] Wang L. Machine availability monitoring and machining process planning towards Cloud manufacturing. *CIRP Journal of Manufacturing Science and Technology* 2013; 6: 263–273.

[3] Mourtzis D. Simulation in the design and operation of manufacturing systems: state of the art and new trends. *International Journal of Production Research* 2020; 58: 1927–1949.

[4] Mourtzis D, Doukas M, Bernidaki D. Simulation in manufacturing: Review and challenges. *Procedia Cirp* 2014; 25: 213–229.

[5] Hill R. A theory of the yielding and plastic flow of anisotropic metals. *Proceedings of the Royal Society of London Series A Mathematical and Physical Sciences* 1948; 193: 281–297.

[6] Phillips A, Sierakowski RL. On the concept of the yield surface. *Acta Mechanica* 1965; 1: 29–35.

[7] Shiratori E, Ikegami K. Experimental study of the subsequent yield surface by using cross-shaped specimens. *Journal of the Mechanics and Physics of Solids* 1968; 16: 373–394.

[8] Ohno N, Wang J-D. Kinematic hardening rules with critical state of dynamic recovery, Part II: application to experiments of ratchetting behavior. *International journal of plasticity* 1993; 9: 391–403.

[9] Hyun S, Lindgren L-E. Simulating a chain of manufacturing processes using a geometry-based finite element code with adaptive meshing. *Finite Elements in Analysis and Design* 2004; 40: 511–528.

[10] Tersing H, Lorentzon J, Francois A, et al. Simulation of manufacturing chain of a titanium aerospace component with experimental validation. *Finite elements in analysis and design* 2012; 51: 10–21.

[11] Afazov SM. Modelling and simulation of manufacturing process chains. *CIRP Journal of Manufacturing Science and Technology* 2013; 6: 70–77.

[12] Lindgren LE, Lundbäck A, Edberg J, et al. Challenges in finite element simulations of chain of manufacturing processes. In: *Materials Science Forum*. Trans Tech Publ, 2013, pp. 349–353.

[13] Britez D, Werda S, Laheurte R, et al. A comparison of different hardening rules on a multi-step global manufacturing process modeling.

[14] Frémond M. The Clausius-Duhem inequality, an interesting and productive inequality. In: *Nonsmooth Mechanics and Analysis*. Springer, 2006, pp. 107–118.

[15] Germain P. The role of thermodynamics in continuum mechanics. In: *Foundations of Continuum Thermodynamics*. Springer, 1973, pp. 317–333.

[16] Chaboche JL, JL C. Viscoplastic constitutive equations for the description of cyclic and anisotropic behaviour of metals.

[17] Armstrong PJ, Frederick CO. *A mathematical representation of the multiaxial Bauschinger effect*. Central Electricity Generating Board [and] Berkeley Nuclear Laboratories …, 1966.

[18] François M. A plasticity model with yield surface distortion for non proportional loading. *International Journal of Plasticity* 2001; 17: 703–717.

[19] Chaboche J-L. Constitutive equations for cyclic plasticity and cyclic viscoplasticity. *International journal of plasticity* 1989; 5: 247–302.

[20] Lemaitre J, Chaboche J-L. *Mechanics of solid materials*. Cambridge university press, 1994.

[21] Besson J, Cailletaud G, Chaboche J-L, et al. *Non-linear mechanics of materials*. Springer Science & Business Media, 2009.

[22] Chaboche J-L. A review of some plasticity and viscoplasticity constitutive theories. *International journal of plasticity* 2008; 24: 1642–1693.

[23] Prager W. The theory of plasticity: a survey of recent achievements. *Proceedings of the Institution of Mechanical Engineers* 1955; 169: 41–57.

[24] Portier L, Calloch S, Marquis D, et al. Ratchetting under tension–torsion loadings: experiments and modelling. *International Journal of Plasticity* 2000; 16: 303–335.

[25] Wu HC, Yeh WC. On the experimental determination of yield surfaces and some results of annealed 304 stainless steel. *International Journal of Plasticity* 1991; 7: 803–826.

[26] Barlat F, Gracio JJ, Lee M-G, et al. An alternative to kinematic hardening in classical plasticity. *International Journal of Plasticity* 2011; 27: 1309–1327.

[27] Calamaz M, Coupard D, Girot F. A new material model for 2D numerical simulation of serrated chip formation when machining titanium alloy Ti–6Al–4V. *International Journal of Machine Tools and Manufacture* 2008; 48: 275–288.

[28] Umbrello D, M'saoubi R, Outeiro JC. The influence of Johnson–Cook material constants on finite element simulation of machining of AISI 316L steel. *International Journal of Machine Tools and Manufacture* 2007; 47: 462–470.

[29] Wang K. *Calibration of the Johnson-Cook failure parameters as the chip separation criterion in the modelling of the orthogonal metal cutting process*. PhD Thesis, 2016.

[30] Pantalé O, Bacaria J-L, Dalverny O, et al. 2D and 3D numerical models of metal cutting with damage effects. *Computer methods in applied mechanics and engineering* 2004; 193: 4383–4399.